Spectrum - The Journal of Operational Applications in Defense Areas

Journal homepage: https://spectrum.ita.br

Electronic Warfare: Counter-UAS

Detection of Drone with Convolutional Neural Network

Vinícius Ormianin Arantes Sousa[1], Kaleb Duarte Costa[2] and Alvaro José Damião[3]

[1]COMPREP, Brasília/DF – Brasil

[2]IAOp, S. José dos Campos/SP – Brasil

[3]IEAv, S. José dos Campos/SP – Brasil

Article Info

Article History:

Received	04 May 2025
Revised	11 June 2025
Accepted	20 July 2025
Available online	23 September 2025

Keywords:

Drone
Detection
CNN
Laser
Infrared

E-mail adresses:

viniciusarantes7@gmail.com
kalebkdc@fab.mil.br
alvdamiao@terra.com.br

Abstract

The increasing use of drones is notable in both military operations and various civilian activities. However, the difficulty in detecting these devices has become a concern when it comes to protecting sensitive areas from unauthorized drone flights. Compounding these challenges is the ability of drones to fly at night, adding an extra layer of difficulty to surveillance and information security efforts. This paper explores the use of an expanded CO_2 laser beam, in a laboratory setting, as an illuminator directed at a drone flying in a controlled environment, aiming to capture images in the long-wave infrared (LWIR) spectrum. The acquired images were used to train a convolutional neural network (CNN) using the YOLO (You Only Look Once) architecture. The results demonstrate the feasibility of using this approach to detect drones when illuminated by an energy source.

I. INTRODUCTION

The use of drones has grown significantly in both military and civilian contexts. This is evidenced by the substantial increase in industries dedicated to manufacturing these aerial platforms. However, the potential misuse of small drones for illicit purposes is also on the rise. In many areas, drone overflights can interfere with critical operations or pose security risks—particularly in military zones, industrial sites, and airports, where protection and confidentiality are essential. Some drones are even capable of transporting warfare items, raising further concerns.

Reports of unauthorized drone flights in restricted areas have led to growing concern among authorities worldwide. To address this issue and minimize illegal drone operations, regulatory bodies responsible for flight safety have intensified their efforts in recent years, introducing increasingly stringent legislation [1].

In this context, the challenge of detecting drones—due to their low radar cross-section (RCS) and minimal electromagnetic emissions—has become a pressing concern for the security and defense of sensitive areas [2][3].

Currently, numerous detection techniques are available for identifying drones in different settings. Visible-spectrum technologies are widely employed, but their performance is limited at night, in cluttered environments, or under adverse weather conditions [4].

To address the challenges of nighttime detection, this study proposes the use of a CO_2 laser beam as an illuminator, aimed at a drone in a controlled flight environment, to capture images in the long-wave infrared (LWIR) spectrum. The LWIR spectrum was chosen for its ability to deliver accurate thermal information, enabling the identification of drones even in low-light conditions or against complex backgrounds.

The images captured with the aid of the laser-based illuminator were used to train a convolutional neural network based on the YOLO architecture [2], which is well-known for its speed and accuracy in real-time object detection tasks. This training aimed to validate the neural network's performance and demonstrate the feasibility of detecting drones when illuminated by a specific energy source, thus offering a promising solution for drone detection in nighttime environments.

By exploring this methodology and considering the existing detection challenges, this study aims to contribute to the development of more effective solutions for nighttime drone detection, enhancing the security of sensitive areas and providing greater protection against potential aerial threats.

II. MATERIALS AND METHODS

In the experiment, a quadcopter drone was used, measuring 27 × 27 × 5.5 cm (Fig. 1). It was tethered to both the floor and ceiling to limit its mobility across all three axes. The drone was suspended using cables, carabiners, and eyelets, maintaining a height of 0.9 m above the ground.

It could move within a range of 0.1 m vertically and 0.3 m horizontally.

Fig. 1. Drone tethered to maintain reduced mobility during flight.

The illuminator used was a Synrad CO_2 laser (Fig. 2), operating at a wavelength of 10.6 µm with a maximum power output of 30 W. During the experiment, the laser operated at 40% of its total power, equivalent to 12 W. The choice of this laser type and wavelength was based on the available equipment.

Despite the constraint, this type of laser is well-suited for heat detection and long-range surveillance. A key characteristic of this laser is its high-power output, which enhances the visibility of reflected infrared radiation. As the laser power increases, the reflectivity on the drone's surface becomes more pronounced, causing the thermal camera to interpret the reflections as variations in surface temperature. This effect enables the identification of multiple thermal “hot spots” across the drone’s body.

Since the laser beam exits with a diameter of approximately 3.5 mm and has a total divergence angle of 4 mrad due to diffraction, an optical system using two plano-convex lenses (Fig. 3) was employed to expand the beam [5]. The drone was positioned 6 meters from the exit point of the second lens (the lens closest to the drone) in the optical assembly.

Fig. 2. 30 W Synrad CO_2 laser with adjustable power output.

Fig. 3. Optical setup with two plano-convex lenses.

To acquire LWIR images, a WIRIS Pro radiometric thermal camera from Workswell was used (Fig. 4). This camera was selected for its sensitivity to wavelengths in the 7.5–13.5 µm range. [6]

Fig. 4. Workswell WIRIS Pro radiometric thermal camera.

The experimental setup, including the laser, camera, and drone positions, is illustrated in Fig. 5.

Image extraction from the recorded videos was performed using ThermoLab software, which allows playback of ".wseq" files generated by the WIRIS Pro camera [6]. The extracted images were annotated using the LabelImg software, which generates ".txt" files containing the object class and coordinates of the bounding boxes.

For data processing and computer vision tasks, two Python libraries were employed: NumPy (Numerical Python), which supports numerical operations such as matrix multiplication and convolutions, and integrates well with the Darknet framework (described below); and OpenCV (Open Source Computer Vision Library), which provides tools for image manipulation, analysis, and visualization of training results.

The convolutional neural network was trained using the YOLOv4 (You Only Look Once, version 4) object detection algorithm. This model resizes images to 448 × 448 pixels, processes them through a single convolutional network, and applies a confidence threshold to determine the presence of objects [7].

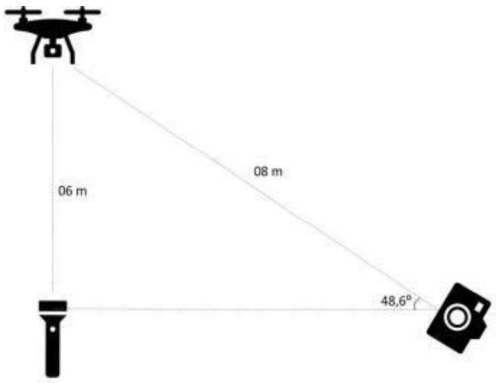

Fig. 5. Schematic diagram of the experimental setup.

The training was conducted using the Darknet deep learning framework, an open-source system written in C and CUDA. To enable GPU-accelerated training, the Google Colaboratory platform was used, which offers high-performance parallel processing capabilities, thereby accelerating the training process and improving efficiency.

At the conclusion of the experiment, the neural network was validated using Visual Studio Code. The software was used to display test images and visually confirm the model’s performance.

If the object of interest was detected, a bounding box with a confidence score was shown; if no object was detected, the image remained unmarked.

III. METHODOLOGY

This experiment aimed to detect signals generated by the reflection of a CO_2 laser beam on a moving drone, using an infrared (IR) camera.

Although object classification was not the primary goal of this study, classification was used as a metric to evaluate the results. The main objective was to detect the laser signal reflected or scattered by the drone, using an infrared camera.

Table I presents the flight phases during which the drone's spectral behavior was evaluated:

a) powered off and not illuminated;
b) powered on and not illuminated;
c) powered on and illuminated by the CO_2 laser;
d) powered off and illuminated by the CO_2 laser;
e) both drone and laser powered off again.

Table I. Phases of experiment

PHASE	DRONE	LASER	TIME VIDEO
1	OFF	OFF	0 to 9.5 S
2	ON	OFF	9.5 to 25 S
3	ON	ON	25 to 45 S
4	OFF	ON	45 to 53 S
5	OFF	OFF	53 to 54 S

Initially, the experiment sought to determine whether a spectral difference could be observed when the drone was illuminated by the laser compared to when it was not. Fig. 6 shows a graph confirming this spectral distinction, as indicated by changes in average and peak temperatures measured by the IR camera.

It was clearly observed that during phases 1 and 2, when the laser was off, the maximum recorded temperature did not exceed 27.7 ºC. In contrast, during phases 3 and 4, when the laser was active and reflecting off the drone, noticeable temperature spikes were detected. In phase 5, once the laser was turned off again, the temperature readings stabilized, not exceeding 29.5 ºC.

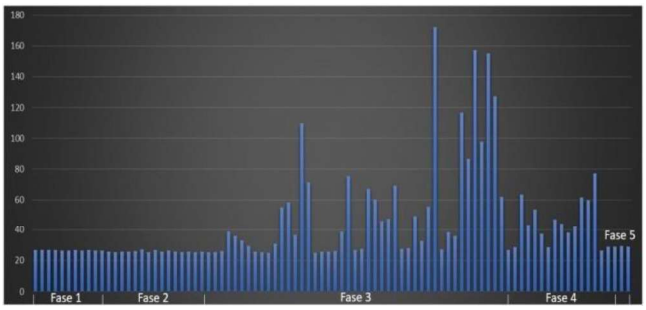

Fig. 6. Temperature in function of time, of agreement with each phase of experiment.

It is important to note that ThermoLab, the software integrated with the Wiris Pro camera, enables temperature-based analysis. However, the temperatures shown do not necessarily reflect the actual surface temperature of the object.

Rather, they represent infrared radiation intensity, which correlates with reflected or absorbed energy. According to Wien's law, this phenomenon describes the relationship between the temperature of a black body and the peak wavelength of its emitted radiation [8]:

$$\lambda_{max} \cdot T = b \tag{1}$$

where b is Wien's displacement constant, approximately 2.897772×10^{-3} m·K

Thus, the temperature values observed correspond to wavelengths emitted or reflected by the drone after being hit by the laser beam. These differences are influenced by surface geometry (e.g., blades, motors, and body), angle of incidence, and material composition (e.g., magnesium alloy, carbon fiber, and composites) [9].

Knowing that the IR signal changes when the drone is illuminated, the maximum temperature recorded prior to laser activation (27.7 ºC) was used to define a threshold. Based on this, the ThermoLab display was adjusted to emphasize regions exceeding that threshold. Fig. 7 shows the unfiltered IR image, while Fig. 8 presents the same frame with the temperature range adjusted to highlight regions above 27.7 ºC.

This temperature adjustment functions similarly to a band-pass optical filter, suppressing signals below the threshold (i.e., unilluminated drone) and revealing only the thermal signal from laser illumination, which corresponds to infrared radiation at 10.6 μm.

From a 55-second video, a total of 98 frames were extracted and used to build the dataset: 69 images for training, 15 for validation, and 14 for testing, as shown in Table II. Given that the YOLO architecture uses pretrained weights, this dataset size was considered acceptable. Had the network been trained from scratch, a larger dataset would have been required.

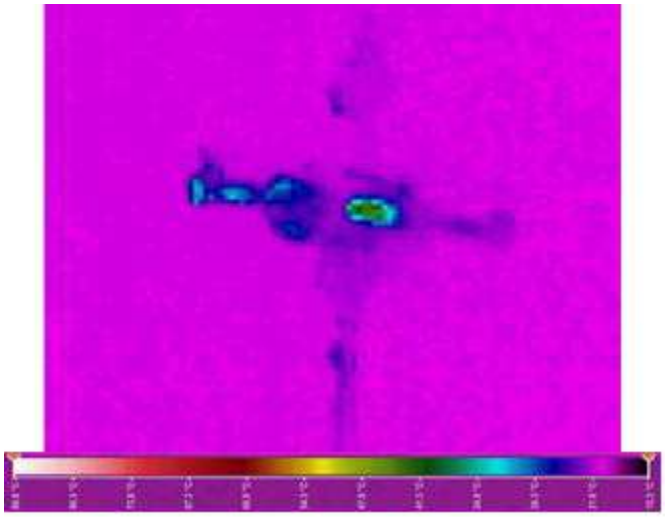

Fig. 7. Drone illuminated by CO_2 laser, without scale adjustment temperature.

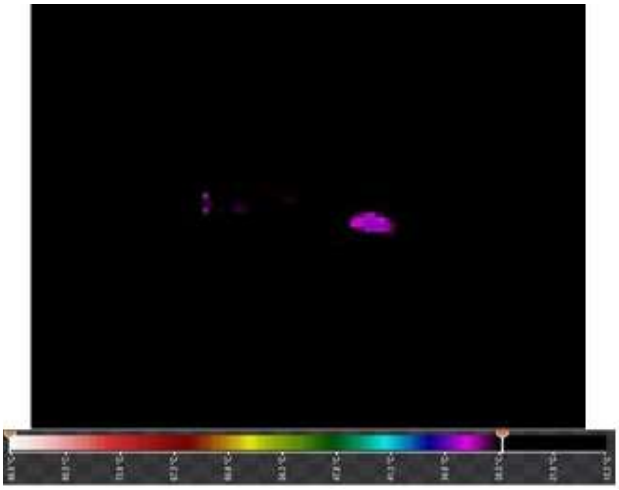

Fig. 8. Drone illuminated for the laser of CO_2 with adjustment in the scale of temperature, above 27.7 ºC.

The dataset was divided following proportions commonly reported in the literature: 70% for training, 15% for validation, and 15% for testing [10][11].

Table II. Division of the images used node training, validation and testing of the convolutional neural network.

Step	Images	Percentage
Training	69	70,4%
Validation	15	15,3%
Testing	14	14,3%

All images were manually annotated using the LabelImg tool. The "drone" label was applied to regions of the drone illuminated by the laser (above 27.7 ºC), while the "non-drone" label was used for visible elements not part of the drone (e.g., cables, hooks, eyelets).

Once labeled, training of the convolutional neural network began and lasted for 4,000 epochs, totaling 14 hours and 45 minutes.

At the end of training, performance was evaluated using the mAP (mean Average Precision) metric, which measures both the precision (accuracy of detections) and recall (ability to detect all relevant objects). As shown in Fig. 9, the loss decreased below 1% after 1,080 epochs (blue curve), while average precision (red curve) ranged from 85% to 100%, ending at 85%. Detection time per image was approximately 1 second.

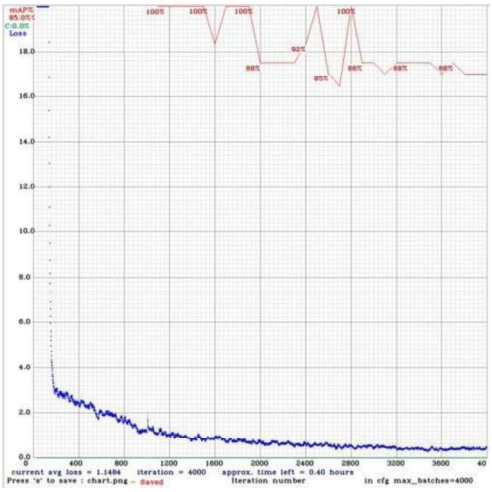

Fig. 9. Performance from the network neural in the training, observed for the function from the error rate (loss) in blue, as a function of training epochs. In red, still, and possible to accompany the average of precision between the classes.

Table III summarizes training performance, including average precision for both classes ("drone" and "non-drone"), overall mAP, and IoU (Intersection over Union), which measures the overlap between predicted and actual bounding boxes. Additional metrics include:

- Precision: 100% – All predictions were correct at a 0.25 confidence threshold.
- Sensitivity (Recall): 67% – 67% of actual drone instances were correctly identified.
- F1 Score: 80% – Harmonic mean of precision and recall.

Table III. Information after end of training.

Class	AP	Pr	Rc	F1 Score	IoU (%)
Drone	100%	1.00	0.67	0.80	73.2
Non-drone	70%	-	-	-	-
mAP	**85%**	-	-	-	-

The average class-wise precision was 100% for “drone” and 70% for “non-drone”.

Because this study focuses on the detection of the presence or absence of a signal, rather than precise object localization, metrics such as sensitivity, precision, and F1 score were prioritized over positional accuracy [12].

In the final testing phase, the trained neural network was activated to evaluate detection on the remaining 14 images (see Table II). Out of these, 10 images showed at least one detection, totaling 16 detections overall (71.5% of the test set). Four images (28.5%) had no detections and were excluded from metric analysis. Table IV summarizes the results of the testing phase, including the total number of detections, classification accuracy, and model confidence scores.

Of the 16 detections, 13 were correct and 3 incorrect. The model-assigned confidence scores for correct detections ranged from 0.54 to 0.96, with an average confidence of 0.71. Fig. 10 illustrates the bounding boxes with class labels and associated confidence scores.

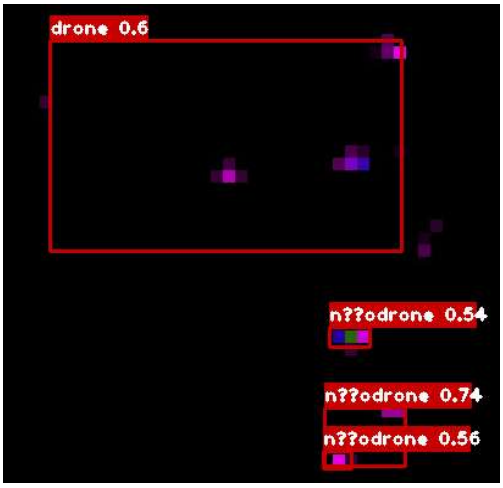

Fig. 10. Example of result presented in the testing from the network neural convolutional.

Table IV. Degree of trust of model to each detection

	Correct Detection		Incorrect Detection	
	Drone	No Drone	Drone	No Drone
Degree of confidence	0.68	0.54	0.71	0.93
	0.64	0.74		0.95
	0.60	0.56		
	0.62	0.96		
	0.81			
	0.66			
	0.90			
	0.72			
	0.90			

Fig. 11 presents a sequence of correctly detected images, including both valid drone regions and non-drone areas, demonstrating the network's capability and potential limitations.

In Fig. 12, you can see the two images that presented signals but were classified incorrectly.

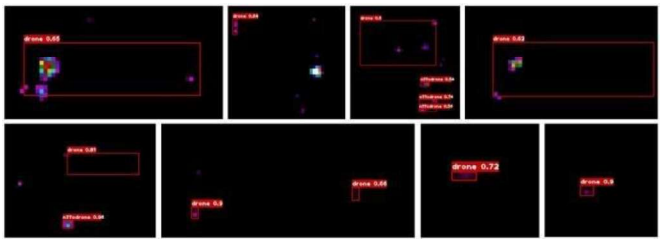

Fig. 11. Junction of all to the images what presented detection and correct classification of objects.

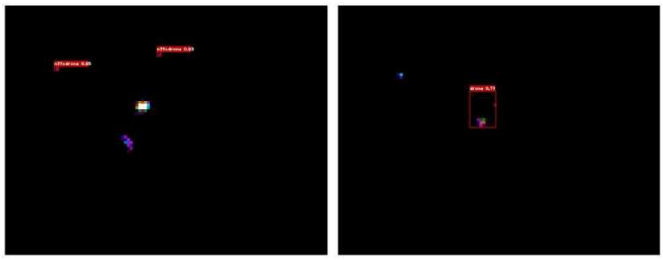

Fig. 12. Images what presented signs incorrectly classified.

IV. FINAL OBSERVATIONS

Based on the analysis of the results obtained, the capabilities of the Wiris Pro infrared camera stand out. When used in combination with the Thermolab software, it allows the setting of upper and lower temperature thresholds of interest, acting similarly to a band-pass optical filter. This configuration highlights the reflectivity of the CO_2 laser on the drone's surface.

Considering that values above 0.8 for recall (sensitivity), and above 0.7 for precision and F1-score are typically considered satisfactory in the literature, the training results can be deemed acceptable for the available dataset.

Given the positive training results, the validation stage is also promising, with more than 70% of the test images showing some form of signal detection and an average confidence level of 70% in the model's predictions.

The results suggest that, with a larger dataset and drone flights conducted without anchoring (i.e., truly free flight), the neural network could be trained even more effectively. This would result in a higher-quality dataset, reducing the likelihood of false positives and improving the model's generalization ability.

Using the proposed methodology, future experiments can be conducted in outdoor environments, varying the distance and flight profiles so that the drone intersects the expanded laser beam. This could increase the chances of obtaining strong reflective signals that are detectable by the infrared sensor. Another improvement would be to capture images with the camera in motion. Depending on its resolution and ability to maintain image quality while tracking, it may be possible to validate the network with a moving camera that follows the drone.

Further enhancement of the detection process could also be achieved by implementing more recent object detection algorithms, such as YOLOv5, which has demonstrated improved performance metrics over YOLOv4 [13].

In conclusion, after analyzing the data obtained through training, validation, and testing of the neural network, it is possible to confirm the feasibility of using this approach for drone detection when illuminated by an external energy source. This method could enhance drone detection, especially in nighttime scenarios or environments with visually complex backgrounds.

REFERENCES

[1] Brazilian Air Force (FAB). "DECEA updates drone access regulations in Brazilian airspace," Brasília, 2023. [Online]. Available: https://www.fab.mil.br. Accessed: Jul. 6, 2023.

[2] S. Singha and B. Aydin, "Automated drone detection using YOLOv4," Drones, vol. 5, no. 3, p. 95, 2021.

[3] V. Dewangan, A. Saxena, R. Thakur, and S. Tripathi, "Application of image processing techniques for UAV detection using deep learning and distance-wise analysis," Drones, vol. 7, no. 3, p. 174, 2023.

[4] M. Misbah, M. U. Khan, Z. Yang, and Z. Kaleem, "TF-net: Deep learning empowered tiny feature network for night-time UAV detection," in Proc. Int. Conf. Wireless and Satellite Systems, Springer, 2023, pp. 3–18.

[5] Synrad (An Excel Technology Company), Series L48 Lasers Operator's Manual, Mukilteo, WA, USA, 2010.

[6] Workswell, Workswell Wiris Pro: User Manual, Czech Republic, FW ver. 1.3.8, 2020.

[7] J. Redmon et al., "You only look once: Unified, real-time object detection," in Proc. IEEE Conf. Comput. Vis. Pattern Recognit., 2016, pp. 779–788.

[8] G. C. Birch and B. L. Woo, "Counter-UAS testing: Evaluation of VIS, SWIR, MWIR and LWIR passive imagers." [Online]. Available: https://www.osti.gov/servlets/purl/1342469. Accessed: Aug. 28, 2023.

[9] D. Höche et al., "Novel magnesium-based materials: Are they reliable drone construction materials?," Frontiers in Materials, vol. 8, Apr. 2021.

[10] S. Sambolek and M. Ivašić-Kos, "Automatic person detection in search and rescue operations using deep CNN detectors," IEEE Access, vol. 9, pp. 37905–37922, 2021.

[11] I. Martinez-Canaryseed et al., "Search and rescue operations using UAVs: A case study," Expert Syst. Appl., vol. 178, p. 114937, 2021.

[12] F. Eick, "Evaluation of convolutional neural network for automatic people detection in aquatic environments using infrared images," M.Sc. thesis, ITA, Brazil.

[13] B. Aydin and S. Singha, "Drone detection using YOLOv5," Eng., vol. 4, no. 1, pp. 416–433, 202.